

## Modelling growth and reproduction of the Pacific oyster *Crassostrea gigas*: Advances in the oyster-DEB model through application to a coastal pond

Y. Bourlès<sup>a,b</sup>, M. Alunno-Bruscia<sup>a,b,\*</sup>, S. Pouvreau<sup>a</sup>, G. Tollu<sup>b</sup>, D. Leguay<sup>b,c</sup>, C. Arnaud<sup>b,c</sup>, P. Gouilletquer<sup>d</sup> and S.A.L.M. Kooijman<sup>e</sup>

<sup>a</sup> Ifremer Station Expérimentale d'Argenton, 11 Presqu'île du Vivier, 29840 Argenton-en-Landunvez, France

<sup>b</sup> CRELA UMR 6217, Place du Séminaire, BP 5, 17137 L'Houmeau, France

<sup>c</sup> UMS-ELA Place Gaby Coll et Allée Hubert Curien BP 5, 17137 L'Houmeau, France

<sup>d</sup> Ifremer Nantes, rue de l'Île d'Yeu, BP 21105, 44311 Nantes Cedex 03, France

<sup>e</sup> Vrije Universiteit, Faculty of Earth and Life Sciences, Department of Theoretical Biology, de Boelelaan 1085, 1081 HV Amsterdam, The Netherlands

\*: Corresponding author : M. Alunno-Bruscia, Tel.: +33 2 98 89 53 93; fax: +33 2 98 89 53 77, email address : [Marianne.Alunno.Bruscia@ifremer.fr](mailto:Marianne.Alunno.Bruscia@ifremer.fr)

### Abstract:

A bio-energetic model, based on the DEB theory exists for the Pacific oyster *Crassostrea gigas*. Pouvreau et al. [Pouvreau, S., Bourlès, Y., Lefebvre, S., Gangnery, A., Alunno-Bruscia, M., 2006. Application of a dynamic energy budget model to the Pacific oyster, *C. gigas*, reared under various environmental conditions. J. Sea Res. 56, 156–167.] successfully applied this model to oysters reared in three environments with no tide and low turbidity, using chlorophyll *a* concentration as food quantifier. However, the robustness of the oyster-DEB model needs to be validated in varying environments where different food quantifiers reflect the food available for oysters, as is the case in estuaries and most coastal ecosystems. We therefore tested the oyster-DEB model on *C. gigas* reared in an Atlantic coastal pond from January 2006 to January 2007. The model relies on two forcing variables: seawater temperature and food density monitored through various food quantifiers. Based on the high temperature range measured in this oyster pond (3–30 °C), new boundary values of the temperature tolerance range were estimated both for ingestion and respiration rates. Several food quantifiers were then tested to select the most suitable for explaining the observed growth and reproduction of *C. gigas* reared in an oyster pond. These were: particulate organic matter and carbon, chlorophyll *a* concentration and phytoplankton enumeration (expressed in cell number per litre or in cumulative cell biovolume). We conclude that when phytoplankton enumeration was used as food quantifier, the new version of oyster-DEB model presented here reproduced the growth and reproduction of *C. gigas* very accurately. The next step will be to validate the model under contrasting coastal environmental conditions so as to confirm the accuracy of phytoplankton enumeration as a way of representing the available food that sustains oyster growth.

**Keywords:** DEB theory; Modelling; Bivalves; *Crassostrea gigas*; Food Quantifiers; Temperature Effect; Coastal Environment

## 1. Introduction

Energetic budget models have been widely applied to bivalves in aquaculture, especially for assessing the carrying capacity of coastal systems (e.g. [Héral, 1993], [Dowd, 1997], [Bacher et al., 1998], [Duarte et al., 2003] and [Grant et al., 2003]). Such models are based on ecophysiological modelling that details the physiological processes and energetics of an organism in response to environmental fluctuations. Most energetic models of bivalves are net production models (e.g. [Ross and Nisbet, 1990], [Raillard et al., 1993], [Smaal and Widdows, 1994], [Barillé et al., 1997], [Campbell and Newell, 1998], [Grant and Bacher, 1998], [Scholten and Smaal, 1998], [Ren and Ross, 2001], [Hawkins et al., 2002] and [Gangnery et al., 2003]) based on the Scope for Growth (SFG) concept (Bayne and Newell, 1983). Dynamic energy budget (DEB) models are a different type of energetic model that describes the rates at which organisms assimilate and utilise energy for maintenance, growth and reproduction. DEB modelling has also been applied to various bivalves (e.g. [Van Haren and Kooijman, 1993], [Ren and Ross, 2005], [Cardoso et al., 2006] and [Pouvreau et al., 2006]). The DEB theory is based on physical and chemical assumptions for individual energetics ([Kooijman, 1986] and [Kooijman, 2000]), whereas the energetics in SFG models are empirically-based using allometric relationships ([Lika and Nisbet, 2000], [Nisbet et al., 2000] and [Van der Meer, 2006]).

DEB theory has recently been more specifically applied to the Pacific oyster *Crassostrea gigas* (e.g. Van der Veer and Alunno-Bruscia, 2006 H.W. Van der Veer and M. Alunno-Bruscia, The DEBIB project: dynamic energy budgets in bivalves, *J. Sea Res.* 56 (2006), pp. 81–84. Article | PDF (91 K) | View Record in Scopus | Cited By in Scopus (1)Van der Veer and Alunno-Bruscia, 2006). Pouvreau et al. (2006) validated the DEB model for this species reared in various different environments and concluded that the model could be applied in many ecosystems where *C. gigas* is cultured. Our study aims to refine the initial version of the oyster-DEB model by Pouvreau et al. (2006) and to test the updated version under new environmental conditions in an Atlantic oyster pond. More precisely, this paper describes how effects of temperature on physiological processes have been modified and improved in the model, compared with the extended Arrhenius

## 1. Introduction

Energetic budget models have been widely applied to bivalves in aquaculture, especially for assessing the carrying capacity of coastal systems (e.g. [Héral, 1993], [Dowd, 1997], [Bacher et al., 1998], [Duarte et al., 2003] and [Grant et al., 2003]). Such models are based on ecophysiological modelling that details the physiological processes and energetics of an organism in response to environmental fluctuations. Most energetic models of bivalves are net production models (e.g. [Ross and Nisbet, 1990], [Raillard et al., 1993], [Smaal and Widdows, 1994], [Barillé et al., 1997], [Campbell and Newell, 1998], [Grant and Bacher, 1998], [Scholten and Smaal, 1998], [Ren and Ross, 2001], [Hawkins et al., 2002] and [Gangnery et al., 2003]) based on the Scope for Growth (SFG) concept (Bayne and Newell, 1983). Dynamic energy budget (DEB) models are a different type of energetic model that describes the rates at which organisms assimilate and utilise energy for maintenance, growth and reproduction. DEB modelling has also been applied to various bivalves (e.g. [Van Haren and Kooijman, 1993], [Ren and Ross, 2005], [Cardoso et al., 2006] and [Pouvreau et al., 2006]). The DEB theory is based on physical and chemical assumptions for individual energetics ([Kooijman, 1986] and [Kooijman, 2000]), whereas the energetics in SFG models are empirically-based using allometric relationships ([Lika and Nisbet, 2000], [Nisbet et al., 2000] and [Van der Meer, 2006]).

DEB theory has recently been more specifically applied to the Pacific oyster *Crassostrea gigas* (e.g. Van der Veer and Alunno-Bruscia, 2006 H.W. Van der Veer and M. Alunno-Bruscia, The DEBIB project: dynamic energy budgets in bivalves, *J. Sea Res.* 56 (2006), pp. 81–84. Article | PDF (91 K) | View Record in Scopus | Cited By in Scopus (1)Van der Veer and Alunno-Bruscia, 2006). Pouvreau et al. (2006) validated the DEB model for this species reared in various different environments and concluded that the model could be applied in many ecosystems where *C. gigas* is cultured. Our study aims to refine the initial version of the oyster-DEB model by Pouvreau et al. (2006) and to test the updated version under new environmental conditions in an Atlantic oyster pond. More precisely, this paper describes how effects of temperature on physiological processes have been modified and improved in the model, compared with the extended Arrhenius

1 relationship proposed by Van der Veer et al. (2006). Model simulations were performed using  
2 a number of food quantifiers to identify those most suitable for predicting the growth of *C.*  
3 *gigas*. In the initial oyster-DEB model by Pouvreau et al. (2006), chlorophyll *a* concentration  
4 (chl-*a*) was the only food quantifier tested. Although chl-*a* is often used to estimate the  
5 phytoplankton biomass available for filter-feeders, there are many sources of discrepancies  
6 when using chl-*a*: (1) quantity of chl-*a* per phytoplankton cell varies a great deal over the year  
7 (Llewellyn et al., 2005), (2) the chl-*a* measured includes inputs from many sources, *e.g.* from  
8 macroalgae and river detritic particles containing both labile and refractory components, toxic  
9 algae, and picoplankton such as Chlorophyta flagellates, which are not retained or assimilated  
10 by *C. gigas* (Barillé et al., 1993, Dupuy et al., 2000b). Moreover, chl-*a* is a photosynthetic  
11 pigment and not a nutritive compound for filter-feeders. We therefore tested additional food  
12 quantifiers: particulate organic matter (POM), particulate organic carbon (POC) and, for the  
13 first time to our knowledge, phytoplankton enumeration expressed both in cell number per  
14 litre and in cumulative biovolume of cells. This assessment aimed to determine the most  
15 relevant quantifier to explain oyster growth and reproduction throughout the year.

16

## 17 **2. Material and methods**

### 18 **2.1. Model description**

19 A detailed description of the DEB model validated for *C. gigas* is given in Pouvreau et al.  
20 (2006). The general framework of the oyster DEB model, *i.e.* the equations and most of the  
21 DEB parameters, was kept similar in the present study and hence only a brief summary of the  
22 main outline is presented here. The present study, however, focuses on new improvements  
23 concerning the temperature effect on oyster physiology and the choice of the most relevant  
24 food quantifier.

#### 25 *2.1.1 Model design*

26 The DEB model assumes that the energy which is assimilated through ingested food is  
27 first stored in a reserve compartment. A fixed fraction  $\kappa$  of the energy flux from reserves is  
28 then used for growth and somatic maintenance (plus heating in endothermic animals), with a  
29 priority for maintenance. The remaining energy fraction  $(1-\kappa)$  is spent on maturity  
30 maintenance and maturation in embryos and juveniles or reproduction, *i.e.* gamete production  
31 and spawning, in adults. DEB parameter values are taken from Pouvreau et al. (2006) (Table

1) Notation and symbols follow Kooijman (2000). Quantities are expressed per unit of structural volume with square brackets [], or per unit of surface-area of the structural body volume with braces {}. All rates have dots, indicating the dimension per time.

The energy ingestion rate  $\dot{p}_X$  is proportional to the surface area of the structural body volume  $V^{2/3}$  and depends upon food density  $X$  in the environment by a Holling type II functional response:

$$\dot{p}_X = \{\dot{p}_{Xm}\} f V^{2/3}, \text{ with } f = \frac{X}{X + X_K} \quad (\text{J d}^{-1}) \quad (1)$$

where  $\{\dot{p}_{Xm}\}$  is the maximum ingestion rate per unit of surface area and  $f$  is the dimensionless functional response which can vary between 0 and 1.  $X_K$  is the saturation coefficient, or Michaelis-Menten constant. It is the food density at which the ingestion rate is half the maximum. The assimilation rate  $\dot{p}_A$  is given as:

$$\dot{p}_A = \{\dot{p}_{Am}\} f V^{2/3} \quad (\text{J d}^{-1}) \quad (2)$$

where  $\{\dot{p}_{Am}\}$  is the maximum surface-area-specific assimilation rate. Its precise value depends on the oyster diet. The ratio  $\{\dot{p}_{Am}\}/\{\dot{p}_{Xm}\}$  gives the conversion efficiency of ingested food into assimilated energy, known as the assimilation efficiency  $AE$  called  $\kappa_A$  in the DEB theory.

Assimilation rate  $\dot{p}_A$  contributes to the energy reserve dynamics given by:

$$\frac{dE}{dt} = \dot{p}_A - \dot{p}_C \quad (\text{J d}^{-1}) \quad (3)$$

where  $\dot{p}_C$  is the utilisation rate of the reserve energy.

The kappa rule ( $\kappa$ ) states that a fixed fraction of  $\dot{p}_C$  is allocated to somatic maintenance and growth. Maintenance rate  $\dot{p}_M$  is proportional to the structural volume  $V$ , so  $\dot{p}_M = [\dot{p}_M] V$ , with  $[\dot{p}_M]$  the maintenance cost per unit of volume. Therefore, the structural body volume  $V$  changes as:

$$\frac{dV}{dt} = (\kappa \cdot \dot{p}_C - \dot{p}_M) / [E_G] \quad (\text{cm}^3 \text{ d}^{-1}) \quad (4)$$

where  $[E_G]$  denotes the volume-specific costs for structure. Kooijman (2000, chapter 3.4) showed that  $\dot{p}_C$ , the energy consumed (fixed and dissipated) by the body tissues, can be written as:

$$\dot{p}_C = \frac{[E]}{[E_G] + \kappa [E]} \left( \frac{[E_G] \{\dot{p}_{Am}\} V^{2/3}}{[E_m]} + [\dot{p}_M] V \right) \quad (\text{J d}^{-1}) \quad (5)$$

1 where  $[E]$  represents the energy density and equals  $E/V$ , and  $[E_m]$  is the maximum energy  
 2 density in the reserve compartment. Thus,  $[E]$  can vary between 0 and  $[E_m]$ .

3 As  $\kappa$  is the fraction of the energy utilisation rate  $\dot{p}_c$  spent on somatic maintenance plus  
 4 growth, the remaining  $(1-\kappa)\dot{p}_c$  is allocated to maturity maintenance and maturity in embryos  
 5 and juveniles, or reproduction (*i.e.* gamete production and spawning) in adults. If the somatic  
 6 and maturity maintenance rate coefficients are equal, the maturity maintenance  $\dot{p}_j$  is  
 7 proportional to the structure  $V$  until juveniles reach sexual maturity at volume  $V_P$ . Maturity  
 8 maintenance does not increase beyond this level. Thus,  $\dot{p}_j$  is defined as:

$$9 \quad \dot{p}_j = \left( \frac{1-\kappa}{\kappa} \right) \text{Min}(V, V_P) [\dot{p}_M] \quad (\text{J d}^{-1}) \quad (6)$$

10 The dynamics for energy allocated first to maturation in juveniles, and then to the  
 11 reproduction buffer  $E_R$  in adults are:

$$12 \quad \frac{dE_R}{dt} = (1-\kappa)\dot{p}_c - \dot{p}_j \quad (\text{J d}^{-1}) \quad (7)$$

13 Shell length  $L$  (cm) is proportional to the structural body volume  $V$ :

$$14 \quad L = \frac{V^{1/3}}{\delta_m} \quad (\text{cm}) \quad (8)$$

15 where  $\delta_m$  is the dimensionless shape coefficient, estimated at 0.175 by Van der Veer et al.  
 16 (2006), Pouvreau et al.(2006) and Bacher and Gangnery (2006) who each used independent  
 17 datasets.

### 18 2.1.2. Temperature effect (the Arrhenius relationship)

19 Physiological processes, *e.g.* assimilation, maintenance and structural growth in the DEB  
 20 model, depend on the body temperature. Within a species-specific temperature tolerance  
 21 range, physiological rates increase exponentially with temperature, as described by the  
 22 Arrhenius relation:

$$23 \quad \dot{k}(T) = \dot{k}_1 \cdot \exp \left\{ \frac{T_A - T_A}{T_1 - T} \right\} \quad (9)$$

24 where  $\dot{k}(T)$  is a physiological rate at ambient temperature  $T$  (in K),  $\dot{k}_1$  is its value at a chosen  
 25 reference temperature  $T_1$ , and  $T_A$  is the Arrhenius temperature (in K) similar for all  
 26 physiological rates of an animal. The basic Arrhenius correction  $\exp \left\{ \frac{T_A - T_A}{T_1 - T} \right\}$  is applied in the  
 27 description of temperature effect on physiological processes, giving 1 when  $T=T_1$ . For *C.*  
 28 *gigas*,  $T_1$  is commonly given at 20°C. Outside the optimal temperature boundaries defined as

1  $T_L$  (lower boundary) and  $T_H$  (upper boundary), *i.e.* at both low ( $T < T_L$ ) and high ( $T > T_H$ )  
 2 temperatures, physiological rates drop quickly (Fig. 1). In the DEB theory,  $T_L$  and  $T_H$  are  
 3 assumed to be the same for all physiological rates. To take into account both boundaries,  
 4 equation (9) can be re-written with the extensive Arrhenius relationship:

$$5 \quad \dot{k}(T) = k_1 \cdot \exp\left\{\frac{T_A - T}{T_1}\right\} \cdot \left(1 + \exp\left\{\frac{T_{AL} - T}{T_L}\right\} + \exp\left\{\frac{T_{AH} - T}{T_H}\right\}\right) \quad (10)$$

6 where  $T_{AL}$  and  $T_{AH}$  are the Arrhenius temperatures (in K) for the rate of decrease at each  
 7 boundary. For *C. gigas*,  $T_L$  and  $T_H$  were respectively estimated at 8°C and 32°C (Van der Veer  
 8 et al., 2006).

9 Values of the temperature tolerance range boundaries  $T_L$  and  $T_H$  were changed in this  
 10 study relative to the initial oyster DEB model (Pouvreau et al., 2006). Two main reasons  
 11 account for this modification. Firstly, the model was previously tested for a temperature range  
 12 from 8 to 25°C (Pouvreau et al., 2006). In many coastal culture sites, such as oyster ponds, the  
 13 seawater temperature can reach extreme values during winter or summer. In our experimental  
 14 oyster pond, seawater temperature varied between 3 and 30°C (see results). Secondly, the  
 15 DEB theory states that within the temperature tolerance range, physiological processes are  
 16 affected in the same way by temperature, *i.e.* that  $T_L$  and  $T_H$  are assumed to be equal for all  
 17 physiological rates (Kooijman, 2000). However, several studies have shown differences in  
 18 temperature effect on feeding processes and respiration rate above a temperature threshold  
 19 (*e.g.* Le Gall and Raillard, 1988; Bougrier et al., 1995; Ren et al., 2000; Hawkins et al., 2002,  
 20 Mao et al., 2006; Le Moullac 2008). Le Gall and Raillard (1988) showed a negative effect of  
 21 high temperature (>25°C) on *C. gigas* growth rate. They explained this depression by a  
 22 change of temperature effect between energy acquisition (food ingestion) which decreased  
 23 significantly at temperatures above 25°C, and energy allocation (metabolism and/or  
 24 maintenance), illustrated by increasing respiration rate above 30°C. Based on physiological  
 25 measurements in acclimated individuals of *C. gigas* over a range of temperature between 5-  
 26 30°C, Bougrier et al (1995) reported increasing oxygen consumption rate from 5 to 30°C and  
 27 increasing clearance rate (food consumption) up to a maximum of 19°C -beyond which the  
 28 clearance rate decreased. Similarly, Ren et al. (2000) modelled the clearance rate of *C. gigas*  
 29 as a hyperbolic function of temperature, with a maximum value at 25°C (like the threshold  
 30 value in Le Gall and Raillard, 1988), whereas oxygen consumption rate increased  
 31 exponentially with temperature. Thus, we assumed that for temperatures above 25°C, oysters  
 32 in our experimental pond neither fed (no assimilation) nor allocated energy to growth and  
 33 maturity. Under this particular condition, respiration could correspond to somatic and

1 maturity maintenance. We thus proposed two new extensive Arrhenius corrections (Fig. 1)  
2 with  $T_L = 3^\circ\text{C}$  for both ingestion and respiration rates, and with  $T_{H\text{ ing}} = 25^\circ\text{C}$  and  $T_{H\text{ resp}} =$   
3  $32^\circ\text{C}$ , respectively for ingestion and respiration rates. Though temperature  $>25^\circ\text{C}$  affected  
4 differently ingestion *vs* respiration rates, the Arrhenius temperature  $T_A$  remained the same for  
5 all physiological rates.

### 6 2.1.3. Food quantifiers

7 The half saturation coefficient  $X_K$  was the only free-fitted parameter of the oyster-DEB  
8 model, as it is supposed to vary according to food quality (Kooijman, 2006), and therefore  
9 according to shellfish growing area. The initial version of the oyster-DEB model used  
10 chlorophyll *a* concentration (chl-*a*) to quantify the trophic resources. In our study, several  
11 more food quantifiers were tested to identify the most suitable one to quantitatively describe  
12 *C. gigas* growth and reproduction. The food quantifiers tested were: chl-*a*, particulate organic  
13 matter (POM) and carbon (POC), and phytoplankton enumeration expressed in cell number  
14 per litre or in cumulative cell biovolume.

## 15 2.2. Environmental and biological data

### 16 2.2.1. Study area

17 The experimental site ‘Marais du Plomb’ is located in the northern part of Marennes-  
18 Oléron Bay (Fig. 2.A). It consists of a series of ponds communicating with the sea by small  
19 channels (Fig. 2.B); no renewal of seawater in the pond occurs for a few days at neap tide.  
20 The ponds are 1 m deep and 200 m<sup>2</sup> in area. Oysters were placed in oyster bags attached to  
21 racks at mid-depth.

### 22 2.2.2. Forcing variables

23 Hydro-biological parameters were monitored in two complementary ways. Temperature  
24 ( $^\circ\text{C}$ ) and chlorophyll *a* concentration (chl-*a* in  $\mu\text{g L}^{-1}$ ) were recorded every 30 min with a  
25 continuous recording multi-parameter detector (DataSonde OTT Hydrolab DS\_5X) immersed  
26 in the vicinity of the oyster racks (1.2 m). Seawater samples were also collected once a week  
27 to quantify particulate organic (POM) and inorganic (PIM) matter, and particulate organic  
28 carbon (POC) and to make phytoplankton identification and enumeration. Samples of seston  
29 for POM, PIM and POC determination were analysed as described in Aminot et al. (2004).



1 Identification and enumeration of phytoplankton species (or groups when identification  
2 was not possible to the species level, *e.g. Euglenophyceae, Pleurosigma+Gyrosigma spp.*)  
3 were done on weekly seawater samples fixed with Lugol's solution (4 mL in 1 L sample).  
4 Size and volume of each species or group were estimated by microscopic analysis, according  
5 to Guillocheau (1988). The phytoplankton *Tetraselmis spp* and *Kryptoperidium foliaceum*,  
6 which showed high blooms and which were respectively reported in the literature as having a  
7 low food value (Robert et al., 2002) and some potentially toxic effects on bivalves  
8 (Landsberg, 2002), were excluded from phytoplankton enumeration to test the model.

### 9 2.2.3. Data validation

10 Five hundred 2-y old oysters were randomly sampled in a large population originating  
11 from Marennes-Oléron Bay. They were deployed in an experimental oyster pond (Fig. 2.B) in  
12 January 2006. Oyster growth was assessed through biometric measurements on 30 oysters  
13 randomly collected on a monthly basis, and every two weeks from June to August, to identify  
14 and quantify spawning events. Oyster dry flesh mass (DFM) was obtained after a 72-hour  
15 freeze-drying cycle and determined to the nearest 0.001 g (Sartorius electronic balance,  
16 precision 0.0001).

## 17 2.3. Model simulations

18 The model was run on STELLA® 8.0 software, using the model parameters from  
19 Pouvreau et al. (2006) and the new boundaries for the temperature tolerance range. The half-  
20 saturation coefficient  $Xk$  was free-fitted for each food quantifier. The coefficients for  
21 conversion of oyster biological components to state variables and processes were taken from  
22 Pouvreau et al. (2006). The initial values of the state variables were as follows: energy in  
23 Structure  $E_V$  was 5000 Joules, energy in Storage  $E$  was 2000 J and energy in the reproduction  
24 buffer  $E_R$  was 2500 J. The structural volume  $V$  was calculated according to length  $L$ , using the  
25 shape coefficient  $\delta$  and the formula  $V=(\delta.L)^3$ , as in Pouvreau et al. (2006). The initial value of  
26 Storage  $E$  and the reproduction buffer  $E_R$  were deduced to obtain the correct initial total dry  
27 mass (0.56 g), as well as realistic initial values for the energy density [E] and gonado-somatic  
28 index GI defined as the ratio between the gonad mass and the total flesh mass (*i.e.* structure,  
29 plus reserve and gonad). Since the temperature effect had been shown to be obviously  
30 different for ingestion and respiration rates, different boundary values of the temperature  
31 tolerance range were applied for each physiological process.

1 The forcing variables used to run the model were the seawater temperature and food  
2 density expressed by the different food quantifiers. Phytoplankton enumeration, expressed in  
3 cell number per litre or in cumulative cell biovolume, was tested as a food quantifier in two  
4 ways: 1/ with the total phytoplankton composition identified and 2/ with only the “selected”  
5 phytoplankton composition, without the two excluded species (see 2.2.2.).

6 Individual growth expressed in dry flesh mass (DFM) was simulated by the model with  
7 each food quantifier and then compared to observed DFM data. For each simulation, the  
8 goodness of fit of the model was estimated by fitting a linear regression between observed  
9 and simulated values, and comparing the resulting slopes and intercept of significant  
10 regressions to 1 and 0, respectively.

## 11 **3. Results**

### 12 **3.1. Forcing variables**

13 Temporal variations in the forcing variables between January 2006 and January 2007 are  
14 illustrated in Figures 3 and 4, for the seawater temperature and food quantifiers, respectively.  
15 Seawater temperature showed a classical seasonal pattern from 3°C to 30°C between January  
16 and July 2006 (Fig. 3). POC varied from 0.2  $\mu\text{g L}^{-1}$  in February to 2.7  $\mu\text{g L}^{-1}$  in May (Fig.  
17 4.A). POM showed a similar pattern to POC, with concentration varying from 2  $\text{mg L}^{-1}$  in  
18 February 2006 to 12  $\text{mg L}^{-1}$  in January 2007 (Fig. 4.B). Chl-a varied between 1  $\mu\text{g L}^{-1}$  in  
19 February and August and 25  $\mu\text{g L}^{-1}$  during spring algal blooms in April (Fig. 4.C). These  
20 three food quantifiers exhibited only three common peaks (1, 2 and 3, Fig. 4) whereas most of  
21 their other peaks were obviously different in terms of magnitude and timing (*e.g.* peaks i to  
22 viii, Fig. 4).

23 The other food quantifier tested in the oyster-DEB model was phytoplankton enumeration  
24 (Fig. 4.D) expressed in cell number ( $\text{cell L}^{-1}$ ) and in cumulative cell volume ( $\mu\text{m}^3 \text{L}^{-1}$ ). The  
25 two expressions of phytoplankton enumeration presented different phytoplankton dynamics,  
26 except for peak 2, which had also been seen in the three first food quantifiers (Fig. 4). When  
27 expressed in number of cells per litre, the total phytoplankton exhibited four high blooms  
28 above  $10^6 \text{cell L}^{-1}$ . The highest ones reached about  $5 \cdot 10^6 \text{cell L}^{-1}$  (September 6th) and  $3.7 \cdot 10^6$   
29  $\text{cell L}^{-1}$  (July 6th). Expressed in their biovolume, some phytoplanktonic blooms corresponded  
30 to those identified by enumeration (in early July and early September), but other blooms were  
31 revealed. Here, the highest blooms reached  $16 \cdot 10^9 \mu\text{m}^3 \text{L}^{-1}$  in late September and about  
32  $13 \cdot 10^9 \mu\text{m}^3 \text{L}^{-1}$  in early July. The gap between blooms expressed in cell number or biovolume

1 is explained by the size variability between species (Table 2.B). Phytoplanktonic cell  
2 biovolume ranged from  $500 \mu\text{m}^3$  for *Tetraselmis sp.* to  $600\,000 \mu\text{m}^3$  for *Flavella sp.*, *i.e.*  
3 interspecific cell size differences could vary by up to 1000 times.

4 More than 100 species or groups of phytoplankton cells were identified in the  
5 experimental oyster pond. Several species, present at low densities but all year long, showed a  
6 high frequency (*e.g. Leptocylindrus sp., Achnantes sp., Amhora sp., Cocconeis sp., Oblea sp.,*  
7 *Prorocentrum sp.*). Despite the high diversity, only a few phytoplanktonic species contributed  
8 to the major part of the density observed through the year. Seven species/groups represented  
9 about 90% of the total cumulative enumeration (Table 2.A). Among them, *Tetraselmis sp.* and  
10 the Class *Euglenophyceae* contributed more than 47%. In terms of biovolume, the ranking  
11 was different with a different set of seven species/groups representing about 83% of the total  
12 cumulative algal biovolume available over the year (Table 2.B). Among these, two species,  
13 *Pleurosigma elongatum* and *Kryptoperidinium foliaceum*, which had respective cell  
14 biovolume of  $150\,000 \mu\text{m}^3 \text{ cell}^{-1}$  and  $30\,000 \mu\text{m}^3 \text{ cell}^{-1}$ , contributed about 53% of the total  
15 phytoplankton biovolume estimated over one year.

### 16 **3.2. Oyster growth**

17 The observed dry flesh mass (DFM) over the year showed two increasing periods, first  
18 between February and June, then from September to January (Fig. 5). In February, there was a  
19 slight decrease of the DFM from 0.75 g to 0.67 g. An important increase of DFM then  
20 occurred in spring and the level reached 3.09 g in late June, probably due to gametogenesis.  
21 During summer a significant decrease was observed until August, with DFM dropping to 1.75  
22 g, most likely due to two processes. Firstly, two spawning events occurred, a massive one in  
23 early July and a minor one in early August. Secondly, no growth was observed at this time.  
24 Oysters did not benefit from the apparently suitable food density level (high POC and POM,  
25 Fig. 4) in July because of the high temperature above  $25^\circ\text{C}$ , which inhibited feeding processes  
26 (see 2.1.2.). In autumn, the DFM again showed a significant increase, reaching more than 3 g  
27 by January 2007.

### 28 **3.3. Growth simulations**

29 The growth of dry flesh mass (DFM) was simulated with the updated version of the  
30 oyster-DEB model, including the improvements incorporated for temperature effects on  
31 physiological processes. For each food quantifier tested, the model was adjusted for the half  
32 saturation coefficient  $X_K$  only as this parameter is diet-specific. The first three food

1 quantifiers, chl-a, POC and POM, commonly used in bivalve nutrition studies, provided the  
2 same simulation pattern, which had no optimal agreement with the observed growth (Fig. 5;  
3 Table 3). These simulations underestimated the observed dry flesh mass in spring and  
4 summer, and over-estimated it for the following winter. The optimised values for  $X_K$  were 9  
5  $\mu\text{g L}^{-1}$ ,  $1.3 \mu\text{g L}^{-1}$  and  $6.4 \text{mg L}^{-1}$ , for chl-a, POC and POM respectively.

6 Phytoplankton enumeration was used as a food quantifier in cell number per litre and in  
7 cumulative cell biovolume, first with the total composition identified throughout the year, and  
8 then with the selected phytoplankton composition only (see 2.1.3). When using the selected  
9 phytoplankton (S-phyto) expressed in cell number, both the magnitude and shape of the  
10 simulated DFM growth trajectories fitted quite well the observed growth (Fig. 6A). Compared  
11 to total phytoplankton composition (Figs. 6C & 6D), S-phyto in cell number led to the best fit  
12 of the regression model between observed and simulated DFM with slope and intercept which  
13 were not significantly different from 1 ( $p$ -value = 0.940) and 0 ( $p$ -value = 0.991) respectively  
14 (Table 3). In contrast, the selected phytoplankton expressed in cell biovolume provided the  
15 same simulation pattern as the first three food quantifiers, with a dry flesh mass  
16 underestimated in spring and summer, and over-estimated in the following winter.  $X_K$  values  
17 were  $1.6 \cdot 10^5 \text{ cell L}^{-1}$  and  $1.4 \cdot 10^9 \mu\text{m}^3 \text{ L}^{-1}$ , for phytoplankton enumeration expressed in cell  
18 number and biovolume respectively (Fig. 6B).

19

## 20 **4. Discussion**

21 In this study, several parameters of the existing oyster-DEB model developed by Pouvreau  
22 et al. (2006) were reconsidered and modified. The resulting second version of the model was  
23 then applied and validated on a new dataset of environmental and growth variables. The  
24 model was run with different food quantifiers, and phytoplankton enumeration demonstrated  
25 its reliability to represent the best the available food explaining observed oyster growth. We  
26 first discuss the food quantifier assessment, then analyse the design of the oyster-DEB model  
27 to explain how environmental parameters affect oyster physiology.

### 28 **4.1. Food quantifier assessment**

29 The half-saturation coefficient  $X_K$ , which describes food ingestion through the functional  
30 response  $f$ , was useful for making a methodical examination of the food quantifiers to  
31 highlight which could best quantitatively explain the growth pattern observed over the year.  
32  $X_K$  was the only free-fitted parameter for each food quantifier tested, as it was diet-specific.

1 The optimal value for chlorophyll *a* concentration (chl-*a*) was 8 µg L<sup>-1</sup>, in accordance with  
2 Pouvreau et al. (2006)  $X_K$  values, which varied from 3 to 17 µg L<sup>-1</sup>.  $X_K$  values for the selected  
3 phytoplankton enumeration were 1.6·10<sup>5</sup> cell L<sup>-1</sup> and 1.4·10<sup>9</sup> µm<sup>3</sup> L<sup>-1</sup> in cell number and in  
4 cumulative cell biovolume respectively. To our knowledge, this is the first time that a half-  
5 saturation coefficient  $X_K$  has been given for oysters fed with natural phytoplankton  
6 enumerated from direct microscopy analyses.

7 The two species removed from the total phytoplankton enumeration were among the most  
8 abundant species whether phytoplankton enumeration was expressed in cell number per litre  
9 (*Tetraselmis sp.*) or in cumulative algal biovolume (*Kryptoperidinium foliaceum*). The  
10 selected phytoplankton data provided a better goodness of fit between observed and simulated  
11 oyster growth than did the total phytoplankton enumeration (Fig. 6, Table 3). It demonstrated  
12 that the two species taken out of the total phytoplankton composition were not a significant  
13 part of the phytoplankton sustaining observed oyster growth, although they were among the  
14 most abundant phytoplankton species. A recent experiment consisting in measuring growth of  
15 *C. gigas* juveniles fed on *Tetraselmis suecica* (monospecific diet) over seven weeks under  
16 controlled conditions showed that oyster ingestion for *T. suecica* was very low and absorption  
17 efficiency almost null, and that no growth in terms of dry flesh mass occurred during the  
18 experiment (Bogolino 2008). In further studies on oyster food availability, the phytoplankton  
19 composition and species dynamics should be analysed and tested with the updated oyster-  
20 DEB model to determine the phytoplankton species that quantitatively contribute to oyster  
21 energetics.

22 Our results showed that selected phytoplankton enumeration in cell number per litre better  
23 represented the available food for oysters than did the same phytoplankton expressed in  
24 cumulative cell biovolume. This result could be explained by the dynamics of phytoplankton  
25 composition, dominated in spring by diatoms and in autumn by large dinoflagellates. Large  
26 dinoflagellates are known to be of poor food quality for bivalves (Landsberg, 2002) and many  
27 taxa are even potentially toxic (*e.g.* Gymnodiniaceae, Dinophyceae). The use of  
28 phytoplankton enumeration expressed in volume over-estimated the contribution of large  
29 dinoflagellates to the available food sustaining oyster energetics, compared with the major  
30 contribution by diatoms. In contrast, phytoplankton enumeration expressed in cell number per  
31 litre was more influenced by the numerous diatoms identified in the oyster pond. Moreover,  
32 cell volume calculation from cell size and shape could increase inaccuracy of cumulative  
33 phytoplanktonic volume estimates.

1 Cell volume and phytoplankton carbon content relationships have been widely studied  
2 (*e.g.* Strathmann, 1967; Montagnes et al., 1994; Menden-Deuer and Lessard, 2000; Cornet-  
3 Barthaux et al., 2007). However, the allometric equations in these previous works were  
4 proposed for broad phytoplanktonic groups. Menden-Deuer and Lessard (2000) gave different  
5 C:volume relationships for diatoms, dinoflagellates and other protist phytoplankton, leading  
6 to global equations that incorporated many uncertainties in phytoplankton carbon estimation.  
7 In coastal ecosystems dominated by a small number of algal blooms (< 10 during the year),  
8 such as the pond ecosystem of our study, specific equations established from species  
9 identification and direct measures (by particle counter for instance) would probably be more  
10 powerful than the previously published general equations relying on estimated volume from  
11 cell size and shape for wide phytoplanktonic groups (diatoms or dinoflagellates).  
12 Furthermore, phytoplankton carbon content evaluation requires extensive environmental  
13 analysis and would therefore not be an easy food quantifier to measure for a model designed  
14 for simple use in diverse environments.

15 Chlorophyll *a* concentration (chl-*a*) has commonly been used to represent either  
16 phytoplankton biomass or the food filtered and digested by bivalves. Recently, Ren and  
17 Schiel (2008) proposed a DEB model specifically designed for *C. gigas* reared in New  
18 Zealand waters, which they validated on chl-*a* data. However, the usefulness of chl-*a* has been  
19 questioned in many studies (*e.g.* Llewellyn et al., 2005; Ren and Ross, 2005; Pouvreau et al.,  
20 2006). In our study, chl-*a*, POC, POM and phytoplankton enumeration were measured. As  
21 reported above, chl-*a* variations were very different from those of phytoplankton enumeration.  
22 Each food quantifier was tested independently. The first three food quantifiers presented the  
23 same pattern through the year (Fig. 4) and produced the same simulations (Fig. 5) with an  
24 underestimation of the dry flesh mass during summer and an overestimation the next winter.  
25 These environmental parameters did not provide good simulations of oyster growth dynamics.  
26 In contrast, the two direct indicators of selected phytoplankton biomass, *i.e.* phytoplankton  
27 enumeration expressed in cell number and in cumulative cell biovolume, provided reasonable  
28 agreements between observed and simulated dry flesh mass (Table 3). These indicators  
29 confirmed that *C. gigas* fed and grew on the available phytoplankton biomass, which was not  
30 well represented by chl-*a* throughout the year under the environmental conditions of our  
31 study. The DEB model designed for *C. gigas* in New Zealand by Ren and Schiel (2008) was  
32 successfully validated on chl-*a* data because the environmental conditions of their study  
33 differed from those in other ecosystems. Seawater temperature, chl-*a* and seston concentration  
34 (TPM) are lower in the New Zealand Sounds, with a smaller range of variation compared with

1 environmental conditions found on French coasts (Ren et al., 2000). Under these specific  
2 conditions, chl-a is a reliable indicator of the phytoplankton available for oysters.

3 Although food quantifiers were tested independently, environmental parameters can affect  
4 more than one simultaneously, *e.g.* the total particulate matter (TPM) influences the clearance  
5 rate and thus the food ingestion. For further development of the oyster-DEB model, feeding  
6 processes should be defined more precisely but without making the model too complex, *i.e.*  
7 by limiting the number of parameters to describe the food acquisition processes (see 4.2. p.  
8 16). As a complementary approach of describing with more details food acquisition in DEB  
9 model, we would recommend to define and test new food quantifiers, *e.g.* the chl-a:C ratio  
10 proposed by Cloern et al. (1995) (see Grangeré et al. 2009 –this issue), which may represent  
11 accurately the food ingested by *C. gigas*. Similarly, a half-saturation coefficient which value  
12 would vary over seasons could improve the accuracy of the food quantifier because seawater  
13 composition is closely related to season; like the sources of chl-a and the dynamics of  
14 phytoplankton composition in the pond ecosystem, dominated by diatoms in spring and by  
15 dinoflagellates in autumn. Finally, using a multivariate functional response as a way to  
16 integrate several food sources is likely a promising approach (Kooijman 2000, p. 160).

17 According to the best simulation obtained, *i.e.* from selected phytoplankton enumeration,  
18 oyster growth dynamics can be described as follows: in February, no growth was observed  
19 due to the low phytoplankton biomass and temperature below 8°C. From March to June, the  
20 high growth of dry flesh mass (DFM) was sustained by several blooms of diatoms and by  
21 increasing temperatures, which rose from 5°C to 25°C. Summer seawater temperatures higher  
22 than 25°C in July affected the dynamics of oyster food uptake. This, in addition to the two  
23 spawning events, explained the decrease of DFM in July, which occurred despite a bloom of  
24 Euglenophyceae. In August, little phytoplankton was detected ( $< 10^5$  cell L<sup>-1</sup>) implying no  
25 growth in DFM. In autumn, oyster growth was again observed. In September and October, the  
26 decreasing temperature (from 25°C to 15°C) remained optimal to sustain an increase of dry  
27 flesh mass from 1.75 g to 2.65 g despite limited available phytoplankton. In contrast,  
28 temperatures were low (from 15°C to 5°C) in November and December, but oyster growth  
29 was sustained by consistent phytoplankton blooms.

#### 30 **4.2. Oyster-DEB model**

31 Some improvements were made to the oyster-DEB model in terms of 1) the effect of  
32 temperature on oyster physiology, 2) the spawning process and 3) the feeding process. First,  
33 the temperature effect on physiological processes was reassessed, with a fine distinction of the

1 rules suggested in the DEB theory (Kooijman, 2000). The abundant literature on bivalve  
2 physiology (*e.g.* Widdows, 1976; Le Gall and Raillard, 1988; Bougrier et al., 1995; Ren et al.,  
3 2000; Hawkins et al., 2002; Mao et al., 2006) underlines the negative effect of temperatures  
4 above 20-25°C on filtration rate, while showing that respiration continues to increase over  
5 30°C. The result for *C. gigas* is a decline in growth rate, or even a loss in weight above 25°C,  
6 whatever the trophic resources. Respiration represents the overall level of metabolic  
7 processes, and at high temperature, respiration rate increase despite a fall of ingestion rate and  
8 so of energy acquisition. Then above 25°C, we considered that respiration could correspond  
9 mainly to maintenance in non feeding (and non-growing) *C. gigas*, thus neglecting all other  
10 contributions (assimilation, overheads of growth and reproduction). The discrepancy between  
11 temperature effect on respiration and ingestion rates was integrated into the updated oyster-  
12 DEB model. Thus, the upper boundaries  $T_H$  of the Arrhenius correction relationship were  
13 25°C and 32°C respectively for ingestion and maintenance rate. According to DEB  
14 assumptions, temperature affects equally all metabolic rates in the temperature tolerance  
15 range which is determined for oyster between 3°C and 25°C. The distinction made in the  
16 oyster-DEB model between energy uptake and use above 25°C illustrated the energetic  
17 deficiency of *C. gigas* in warm water. At the other limit of the temperature tolerance range,  
18 the lower boundary  $T_L$  of the Arrhenius correction relationship was kept similar for the two  
19 functions, at 3°C: a lower value than the 8°C proposed by Van der Veer et al. (2006). The  
20 application of the new temperature tolerance range upper boundaries for ingestion and  
21 maintenance rates, representing the energy acquisition and energy expenditure respectively,  
22 resulted in a slowing down of oyster growth in July, which fits well with biological  
23 observations made at this time, *i.e.* no growth, plus the two spawning events. Preliminary  
24 simulations of the oyster dry flesh mass based on the temperature tolerance range used in  
25 Pouvreau et al. (2006) and on selected phytoplankton enumeration, showed an over-  
26 estimation of DFM in early July (Bourlès, unpublished data). Our finding that temperature  
27 >25°C affects ingestion differently from respiration has no consequence on oyster energetics  
28 in the temperature tolerance range between 3°C and 25°C.

29 The two parameters controlling the spawning events were then also adjusted to allow  
30 several spawnings like those observed during the summer in the oyster pond. The temperature  
31 threshold and gonado-somatic index were free-fitted according to the condition index  
32 observed in reared oysters. They were respectively estimated at 22°C and 40%, which are  
33 slightly higher than the values given by Pouvreau et al. (2006) in the first oyster-DEB model,  
34 (20°C and 35%). This may be explained by the specific environmental quality of the oyster



1 pond which showed high temperature variations and a relatively high food level. Recently,  
2 Ren and Schiel (2008) pointed out that DEB parameter values must be influenced by specific  
3 environmental conditions even if they are supposedly species-specific. Ren and Schiel (2008)  
4 re-estimated the main DEB parameter values from specific experiments on *C. gigas*, but they  
5 validated their DEB model outside the reproductive period, thus avoiding the need to simulate  
6 spawning events. Although it appears difficult to integrate reproductive processes in a bio-  
7 energetic model, these need to be understood and quantified to include the triggering of  
8 spawning events according to given environmental conditions. It is a necessary step to  
9 estimate the quantitative energy budget of *C. gigas* through time, whatever its living  
10 environment, whether this is for aquaculture purposes or for the study of its widening natural  
11 distribution.

12 In our model, energy acquisition was only supported by food ingestion and assimilation.  
13 The model did not take into account the filtration and selection processes which are  
14 commonly integrated into most ecophysiological models (*e.g.* Bacher et al., 1991; Barillé et  
15 al., 1997; Campell and Newell, 1998; Grant and Bacher 1998; Powell et al., 1992; Raillard et  
16 al., 1993; Ross and Nisbet, 1990). The present model assumes a simple Type 2 functional  
17 response. Although total seston and inorganic particles obviously interfere in feeding  
18 processes (Grizzle et al., 2006; Ren et al., 2000), unpublished experimental data on oyster  
19 filtration and ingestion showed that the Type 2 functional response is appropriate for the  
20 Pacific oyster *Crassostrea gigas*. Moreover, energy acquisition in the oyster-DEB model was  
21 built on food quantifiers which represent the food available for oysters. Thus, we chose to  
22 maintain the simple use of the functional response that also has the advantage of involving  
23 few parameters. However, the general feeding model developed by Ren and Ross (2005) is  
24 probably suitable for all bivalve species, and could be investigated to further improve oyster  
25 feeding response to a variable environment. In the recent DEB model validated for *C. gigas*  
26 by Ren and Schiel (2008), the feeding processes were also simplified to the Type 2 functional  
27 response. However these authors also recommended that further refinements of the model  
28 should include the effect of food quantity and quality, *i.e.* the integration of supplementary  
29 environmental variables in addition to the two forcing variables involved in the oyster-DEB  
30 model presented here.

31 Assimilation efficiency was considered as a constant in the present model. Filter-feeders  
32 consume suspended particles composed of a mixture of detrital and phytoplankton organic  
33 matter containing both labile and refractory components. Studies have reported varying  
34 assimilation efficiency with seasonal variations of food quality and phytoplankton

1 composition (Hawkins and Bayne, 1985; Hawkins et al., 1999). However, Ren et al. (2000)  
2 found a constant absorption efficiency of 86% above approximately 5% seston organic  
3 content. Overall, ecophysiological models are usually built with a constant assimilation  
4 efficiency. Ren and Ross (2001, 2005) and Van der Veer et al. (2006) reported an assimilation  
5 efficiency of 75% for various bivalves. Following unpublished experimental data and the first  
6 oyster-DEB model developed by Pouvreau et al. (2006), the same value was used in the  
7 present model.

8

### 9 **4.3. Conclusion**

10 The validation of the new oyster-DEB model demonstrates its suitability for simulating  
11 *Crassostrea gigas* growth and reproduction in rearing sites with broader temperature  
12 variations than the controlled conditions tested by Pouvreau et al. (2006). The updated oyster-  
13 DEB model presented in this paper supports the “aim for generality” of this earlier paper. The  
14 second version of the oyster-DEB model now needs to be tested in different environments  
15 where *C. gigas* grows. Overall, our model has proved to be a useful tool for testing food  
16 quantifiers on a comparative basis. Although several food sources have been identified for  
17 oyster feeding (*e.g.* Deslous-Paoli and Héral, 1984; Barillé et al., 1993; Dupuy et al., 2000a),  
18 it appears that phytoplankton expressed in cell number per litre explains the greater part of  
19 observed oyster growth. The oyster-DEB model could be used as a generic model to further  
20 study *C. gigas* physiology in response to environmental fluctuations (*e.g.* food selection  
21 processes according to food resource quality, and spawning events in relation to summer  
22 temperature and gonad development). The model should also be a powerful tool as part of a  
23 larger ecosystem model to assess carrying capacity of different areas where the Pacific oyster  
24 is cultured.

25

### 26 **Acknowledgements**

27 Y. Bourlès was supported by funding of Région Poitou-Charentes and Ifremer during his PhD  
28 project. We would like to thank two anonymous referees for their helpful comments on the  
29 manuscript. The members of the European Research Group AquaDEB  
30 (<http://www.ifremer.fr/aquadeb/>) are gratefully acknowledged for the stimulating discussions  
31 and useful comments. This paper benefited from helpful comments and English revision by  
32 H. McCombie.

1

## 2 **References**

- 3 Aminot, A., Kerouel, R., Bretaudeau, J., 2004. Marine ecosystem hydrology parameters and  
4 analyses. *Méthodes Anal. Milieu Mar.* 336 pp.
- 5 Bacher, C., Duarte, P., Ferreira, J.G., Héral, M., Raillard, O., 1998. Assessment and  
6 comparison of the Marennes-Oleron Bay (France) and Carlingford Lough (Ireland)  
7 carrying capacity with ecosystem models. *Aquat. Ecol.* 31, 379-394.
- 8 Bacher, C., Héral, M., Deslous-Paoli, J.M., Razet, D., 1991. Modèle énergétique uni-boîte de  
9 la croissance des huîtres (*Crassostrea gigas*) dans le bassin de Marennes-Oléron. *Can. J.*  
10 *Fish. Aquat. Sci.* 48, 391-404.
- 11 Bacher, C., Gangnery, A., 2006. Use of dynamic energy budget and individual based models  
12 to simulate the dynamics of cultivated oyster populations. *J. Sea Res.* 56, 140-155.
- 13 Barillé, L., Prou, J., Héral, M., Bougrier, S., 1993. No influence of food quality, but ration-  
14 dependent retention efficiencies in the Japanese oyster *Crassostrea gigas*. *J. Exp. Mar.*  
15 *Biol. Ecol.* 171, 91-106.
- 16 Barillé, L., Héral, M., Barillé-Boyer, A.L., 1997. Modélisation de l'écophysiologie de l'huître  
17 creuse *Crassostrea gigas* dans un environnement estuarien. *Aquat. Living Resour.* 10, 31-  
18 48.
- 19 Bayne, B.L., Newell, R.C., 1983. Physiological energetics of marine molluscs. In: Saleuddin  
20 A.S.M. , Wilbur K.M. (Eds.), *The Mollusca*, vol. 4. Academic Press, London, pp.407-515.
- 21 Boglino, A. 2008. Les espèces phytoplanctoniques majeures des côtes atlantiques françaises  
22 sont-elles équivalentes pour l'ingestion et la croissance de l'huître creuse (*Crassostrea*  
23 *gigas*) ? Réponse par le biais d'une approche expérimentale. Master 2 report, Sciences de  
24 l'Univers Environnement Ecologie, Pierre & Marie Curie University, Paris 6, 45 p.
- 25 Bougrier, S., Geairon, P., Deslous-Paoli, J.M., Bacher, C., Jonquière, G., 1995. Allometric  
26 relationships and effects of temperature on clearance and oxygen consumption rates of  
27 *Crassostrea gigas* (Thunberg). *Aquaculture* 134, 143-154.
- 28 Campbell, D.E., Newell, C.R., 1998. MUSMOD, a production model for bottom culture of  
29 the blue mussel *Mytilus edulis*. *L. J. Exp. Mar. Biol. Ecol.* 219, 171-203.
- 30 Cardoso, J.F.M.F., Van der Veer, H.W., Kooijman, S.A.L.M., 2006. Body size scaling  
31 relationships in bivalve species: A comparison of field data with predictions by the  
32 Dynamic Energy Budget (DEB) theory. *J. Sea Res.* 56: 125-139.

- 1 Cloern, J.E., Grenz, C., Vidregar-Lucas, L., 1995. An empirical model of the phytoplankton  
2 chlorophyll:carbon ratio-the conversion factor between productivity and growth rate.  
3 *Limn. Oceanogr.* 40, 1313-1321.
- 4 Cornet-Barthaux, V., Armand, L., Quéguiner, B., 2007. Biovolume and biomass estimates of  
5 key diatoms in the Southern Ocean. *Aquat Microb. Ecol.* 48: 205-308.
- 6 Dowd, M., 1997. On predicting the growth of cultured bivalves. *Ecol. Model.* 104, 113-131.
- 7 Deslous-Poali, J.M., Héral, M., 1984. Transferts énergétiques entre l'huître *Crassostrea gigas*  
8 de 1 an et la nourriture potentielle disponible dans l'eau d'un bassin ostréicole. *Haliotis*  
9 14, 79-90.
- 10 Deslous-Poali, J.M., Héral, M., 1988. Biochemical composition and energy value of  
11 *Crassostrea gigas* (Thunberg) cultured in the bay of Marennes-Oléron. *Aquat. Living*  
12 *Resour.* 1: 239-249.
- 13 Duarte, P., Meneses, R., Hawkins, A.J.S., Zhu, M., Fang, J., Grant, J., 2003. Mathematical  
14 modelling to assess the carrying capacity for multi-species culture within coastal waters.  
15 *Ecol. Model.* 168, 109-143.
- 16 Dupuy, C., Pastoureaud, A., Ryckaert, M., Sauriau, P.G., Montanié, H., 2000a. Impact of the  
17 oyster *Crassostrea gigas* on microbial community in Atlantic coastal ponds near La  
18 Rochelle. *Aquat. Microbial Ecol.* 22, 227-242.
- 19 Dupuy, C., Vaquer, A., Lam-Höai, T., Rougier, C., Mazouni, N., Lautier, J., Colloc, Y., Le  
20 Gall, S., 2000b. Feeding rate of the oyster *Crassostrea gigas* in a natural planktonic  
21 community of the Mediterranean Thau Lagoon. *Mar. Ecol. Prog. Ser.* 205, 171-184.
- 22 Grangeré, K., Ménesguen, A., Lefebvre, S., Bacher, C., Pouvreau, S. Modelling the influence  
23 of environmental factors on the physiological status of the Pacific oyster *Crassostrea*  
24 *gigas* in an estuarine embayment; The Baie des Veys (France). *J. Sea Res.* doi: SEARES-  
25 D-08-00109R1 (this issue).
- 26 Gangnery, A., Chariband, J., Lagarde, F., Le Gall, P., Oheix, J., Bacher, C., Buestel, D., 2003.  
27 Growth model of the Pacific oyster *Crassostrea gigas*, cultured in Thau Lagoon  
28 (Méditerranée, France). *Aquaculture* 215, 267-290.
- 29 Grant, J., Bacher, C., 1998. Comparative models of mussel bioenergetics and their validation  
30 at field culture sites. *J. Exp. Mar. Biol. Ecol.* 219, 21-44.
- 31 Grant, J., Archambault, M., Bacher, C., Cranford, P., 2003. Integration of modelling and GIS  
32 in studies of carrying capacity for bivalve aquaculture. *J. Shellfish Res.* 22, 332.

- 1 Grizzle, R.E., Green, J.K., Luckenbach, M.W., Coen, L.D., 2006. A new *in situ* method for  
2 measuring seston uptake by suspension-feeding bivalve molluscs. *J. Shellfish Res.* 25,  
3 643-649.
- 4 Guillocheau, N., 1988. Spatial and temporal distribution of Arcachon Basin phytoplankton.  
5 Ph.D thesis, University of Aix-Marseille, Marseille.
- 6 Hawkins, A.J.S., Bayne, B.L., 1985. Seasonal variation in the relative utilization of carbon  
7 and nitrogen by the mussel *Mytilus edulis*: budgets, conversion efficiencies and  
8 maintenance requirements. *Mar. Ecol. Prog. Ser.* 25, 181-188.
- 9 Hawkins, A.J.S., Duarte, P., Fang, J.G., Pascoe, P.L., Zhang, J.H., Zangh, X.L., Zhu, M.Y.,  
10 2002. A functional model of responsive suspension-feeding and growth in bivalve  
11 shellfish, configured and validated for the scallop *Chlamys farreri* during culture in China.  
12 *J. Exp. Mar. Biol. Ecol.* 281, 13-40.
- 13 Héral, M., 1993. Why carrying capacity models are useful tools for management of bivalve  
14 molluscs culture. In: Dame, R.F. (Ed.), *Bivalve Filter Feeders in Estuarine and Coastal*  
15 *Ecosystem Processes*. Springer-Verlag, Berlin, pp. 455-477.
- 16 Kooijman, S.A.L.M., 1986. Energy budgets can explain body size relations. *J. Theor. Biol.*  
17 121, 269-282.
- 18 Kooijman, S.A.L.M., 2000. *Dynamic energy and mass budgets in biological systems*.  
19 Cambridge Univ. Press, Cambridge.
- 20 Kooijman, S.A.L.M., 2006. Pseudo-faeces production in bivalves. *J. Sea Res.* 56, 103-106.
- 21 Landsberg, J.H., 2002. The effects of harmful algal blooms on aquatic organisms. *Reviews in*  
22 *Fisheries Science* 10, 113-390.
- 23 Le Gall, J.L. Rallard, O., 1988. Influence of temperature on the physiology of the oyster  
24 *Crassostrea gigas*. *Océanis* 14, 603-608.
- 25 Le Moullac, G., 2008. *Adaptation du métabolisme respiratoire de l'huître creuse Crassostrea*  
26 *gigas*. PhD thesis, University of Caen, Caen, 161 pp.
- 27 Lika, K., Nisbet, R.M., 2000. A dynamic energy budget model based on partitioning of net  
28 production. *J. Math. Biol.* 41, 361-386.
- 29 Llewellyn, C.A., Fishwick, J.R., Blackford, J.C., 2005. Phytoplankton community assemblage  
30 in the English Channel: a comparison using chlorophyll *a* derived from HPLC-  
31 CHEMTAX and carbon derived from microscopy cell counts. *J. Plankton Res.* 27, 103-  
32 119.
- 33 Mao, Y., Zhou, Y., Yang, H., Wang, R., 2006. Seasonal variation in metabolism of cultured  
34 Pacific oyster, *Crassostrea gigas*, in Sanggou Bay, China. *Aquaculture* 253, 322-333.

- 1 Menden-Deuer, S., Lessard, E.J., 2000. Carbon to volume relationships for dinoflagellates,  
2 diatoms, and other protist plankton. *Limnol. Oceanogr.* 45(3): 569-579.
- 3 Montagnes, D.J.S., Berges, J.A., Harrison, P.J., Taylor, F.J.R., 1994. Estimating carbon,  
4 nitrogen, protein, and chlorophyll *a* from volume in marine phytoplankton. *Limnol.*  
5 *Oceanogr.* 39(5): 1044-1060.
- 6 Nisbet, R.M., Muller, E.B., Lika, K., Kooijman, S.A.L.M., 2000. From molecules to  
7 ecosystems through dynamic energy budget models. *J. Anim. Ecol.* 69, 913-926.
- 8 Pouvreau, S., Bourles, Y., Lefebvre, S., Gangnery, A., Alunno-Bruscia, M., 2006. Application  
9 of a dynamic energy budget model to the Pacific oyster, *Crassostrea gigas*, reared under  
10 various environmental conditions. *J. Sea Res.* 56, 156-167.
- 11 Powell, E.N., Hofmann, E.E., Klinck, J.M., Ray, S.M., 1992. Modelling oyster populations: a  
12 commentary on filtration rate: is faster always better? *J. Shellfish Res.* 11, 387-398.
- 13 Raillard, O., Deslous-Paoli, J.M., Héral, M., Razet, D., 1993. Modélisation du comportement  
14 nutritionnel et de la croissance de l'huître japonaise *Crassostrea gigas*. *Oceanol. Acta* 16,  
15 73-82.
- 16 Ren, J.S., Ross, A.H., Schiel, D.R., 2000. Functional descriptions of feeding and energetics of  
17 the Pacific oyster *Crassostrea gigas* in New Zealand. *Mar. Ecol. Prog. Ser.* 208, 119-130.
- 18 Ren, J.S., Ross, A.H., 2001. A dynamic energy budget model of the Pacific oyster  
19 *Crassostrea gigas*. *Ecol. Model.* 142, 105-120.
- 20 Ren, J.S., Ross, A.H., 2005. Environmental influence on mussel growth: A dynamic energy  
21 budget model and its application to the greenshell mussel *Perna canaliculus*. *Ecol. Model.*  
22 189, 347-362.
- 23 Ren, J.S., Schiel, D., R., 2008. A dynamic energy budget model: parameterisation and  
24 application to the Pacific oyster *Crassostrea gigas* in New Zealand waters. *J. Exp. Mar.*  
25 *Biol. Ecol.* 361, 42-48.
- 26 Robert, R., Parisi, G., Pastorelli, R., Poli, B.M., Tredici, M., 2002. The food quality of  
27 *Tetraselmis suecica* slurry for *Crassostrea gigas* spat. *Haliotis* 31, 53-56.
- 28 Ross, A.H., Nisbet, R.M., 1990. Dynamic models of growth and reproduction of the mussel  
29 *Mytilus edulis* L. *Funct. Ecol.* 4, 777-787.
- 30 Scholten, H., Smaal, A.C., 1998. Responses of *Mytilus edulis* L. to varying food  
31 concentrations: testing EMMY, an ecophysiological model. *J. Exp. Mar. Biol. Ecol.* 219,  
32 217-239.

- 1 Smaal, A.C., Widdows, J., 1994. The scope for growth of bivalves as an integrated response  
2 parameter in biological monitoring. In: Kramer K. (Ed.), *Biomonitoring of Coastal Waters*  
3 *and Estuaries*. CRC Press, Boca Raton, pp. 247-268.
- 4 Strathmann, R.R., 1967. Estimating the organic carbon content of phytoplankton from cell  
5 volume or plasma volume. *Limnol. Oceanogr.* 12(3): 411-418.
- 6 Van der Meer, J., 2006. Metabolic theories in ecology. *Trends Ecol. Evol.* 21, 136-140.
- 7 Van der Veer, H.W., Alunno-Bruscia, M., 2006. The DEBIB project: Dynamic Energy  
8 Budgets in Bivalves. *J. Sea Res.* 56, 81-84.
- 9 Van der Veer, H.W., Cardoso, J.F.M.F., Van der Meer, J., 2006. The estimation of DEB  
10 parameters for various Northeast Atlantic bivalve species. *J. Sea Res.* 56, 107-124.
- 11 Van Haren, R.J.F., Kooijman, S.A.L.M., 1993. Application of the dynamic energy budget  
12 model to *Mytilus edulis* (L.). *Neth. J. Sea. Res.* 31, 119-133.
- 13 Widdows, J., 1976. Physiological adaptation of *Mytilus edulis* to cyclic temperatures. *J. comp.*  
14 *Physiol.* 105, 115-128.

1 **Tables**

2

3

4 Table 1: DEB parameter values used as in Pouvreau et al. (2006) and values of updated  
5 boundaries of the optimal temperature range for ingestion and respiration rates.

Parameters	Symbol	Units	Value	References
<u>Primary parameters:</u>				
Arrhenius temperature	$T_A$	K	5800	Van der Veer et al. (2006)
Half saturation coefficient	$X_K$	-	-	Free-fitting (cf. food quantifier)
Max. surface area-specific ingestion rate	$\{p_{X_m}\}$	$J\ cm^{-2}\ d^{-1}$	560	Van der Veer et al. (2006)
Assimilation efficiency	$ae$	-	0.75	Van der Veer et al. (2006)
Volume-specific maintenance costs	$[p_m]$	$J\ cm^{-3}\ d^{-1}$	24	Van der Veer et al. (2006)
Maximum storage density	$[E_M]$	$J\ cm^{-3}$	2295	Van der Veer et al. (2006)
Volume-specific costs for structure	$[E_G]$	$J\ cm^{-3}$	1900	Van der Veer et al. (2006)
Structural volume at sexual maturity	$V_p$	$cm^{-3}$	0.4	Pers. unpubl. data
Fraction of $p_C$ spent on maintenance plus growth	$\kappa$	-	0.45	Van der Veer et al. (2006)
Fraction of reproduction energy fixed in eggs	$\kappa_R$	-	0.7	Pouvreau et al. (2006)
Shape coefficient	$\delta_M$	-	0.175	Van der Veer et al. (2006)
<u>Additional parameters:</u>				
Lower boundary of tolerance range	$T_L$	K	281	Van der Veer et al. (2006)
Upper boundary of tolerance range	$T_H$	K	305	Van der Veer et al. (2006)
Rate of decrease at lower boundary	$T_{AL}$	K	75000	Van der Veer et al. (2006)
Rate of decrease at upper boundary	$T_{AH}$	K	30000	Van der Veer et al. (2006)
Energy content of reserves (in ash free dry mass)	$\mu_E$	$J\ mg^{-1}$	17.5	Deslous-Paoli and Héral (1988)
Gonado-somatic index triggering spawning	GI	%	40	Pers. unpubl. data
Temperature threshold triggering spawning	$T_S$	$^{\circ}C$	22	Pers. unpubl. data
<u>New boundary values of the optimal temperature range:</u>				
Lower boundary of tolerance range	$T_L$	K	276	This study
Upper boundary of tolerance range for ingestion	$T_{H\ ing}$	K	298	This study
Upper boundary of tolerance range for respiration	$T_{H\ resp}$	K	305	This study

6

7

8

9

10

11

12



1

2 Table 2.A: Most abundant phytoplankton species identified in the oyster pond from January  
3 2006 to January 2007 in terms of cell number, percentage of the total phytoplankton  
4 enumeration, bloom values and their seasonality.

Species or group	Cumulative cell number	% of total enumeration	Maximum bloom(s) in cell L <sup>-1</sup>	Date (2006)
<i>Tetraselmis sp.</i>	5 233 600	<b>26.9</b>	4 869 000	6 September
<i>Euglenophyceae</i> (Class)	3 953 400	<b>20.3</b>	3 628 400	6 July
Nano-flagellates	2 775 200	<b>14.3</b>	2 143 800	1 June
<i>Chaetoceros spp.</i>	2 067 600	<b>10.6</b>	1 662 000	22 June
<i>Nitzschia longissima</i>	1 492 600	<b>7.7</b>	627 600 / 154 000	20 April / 16 May
<i>Kryptoperidinium foliaceum</i>	1 119 400	<b>5.8</b>	511 000 / 436 000	20 / 29 September
<i>Skeletonema costatum</i>	636 000	<b>3.3</b>	55 800 / 73 200 114 000 / 216 800	14 February / 2 March 16 / 30 March
<b>Total phytoplankton cells</b>	<b>19 452 600</b>			

5

6

7

8 Table 2.B: Phytoplankton with the greatest contribution in terms of cumulative cell volume  
9 estimated in the oyster pond between January 2006 and January 2007 from size and mean  
10 volume (N. Guillocheau, 1988; laboratory measurements in this study). The percentage of the  
11 cumulative cell volume is calculated according the total cumulative cell volume.

Species or group	Size in $\mu\text{m}$ (minimum; maximum)	Mean biovolume ( $\mu\text{m}^3 \text{ cell}^{-1}$ )	Cumulative cell biovolume ( $10^6 \mu\text{m}^3$ )	% of total volume
<i>Kryptoperidinium foliaceum</i>	28x25; 53x51	<b>30 000</b>	33 582	<b>27.5</b>
<i>Pleurosigma elongatum</i>	190x15; 205x20	<b>150 000</b>	30 990	<b>25.4</b>
<i>Euglenophyceae</i> (Class)	24x8; 50x15	<b>3 000</b>	11 860	<b>9.7</b>
<i>Pleurosigma</i> + <i>Gyrosigma</i> spp.	53x13; 700x38	<b>200 000</b>	10 160	<b>8.3</b>
<i>Entomoneis spp.</i>	100x40; 100x55	<b>50 000</b>	8 680	<b>7.1</b>
<i>Flavella sp.</i>	180x72; 196x78	<b>600 000</b>	3 240	<b>2.7</b>
<i>Tetraselmis sp.</i>	8x6; 13x9	<b>500</b>	2 617	<b>2.1</b>
<b>Total cell volume</b>		<b>6 200</b>	<b>122 133</b>	

12

13

14

15

1  
2  
3  
4  
5  
6  
7  
8  
9  
  
10  
11  
12  
13  
14

Table 3: Ordinary least square regression of observed against modelled dry flesh mass of *C. gigas* for the seven simulations carried out with each food quantifier, *i.e.* Chl-a (chlorophyll *a*), POC (particulate organic carbon), POM (particulate organic matter), phyto (phytoplankton), S-phyto (selected phytoplankton). Both phyto and S-phyto are expressed in terms of cell number or cumulative biovolume.  $R^2$ , coefficient of determination and corresponding  $p$ -value on null hypothesis. Slope and intercept values are given for each regression model, with corresponding  $p$ -values of testing slopes different from 1 and intercept different from 0.

Regression parameters	Chl-a	POC	POM	Phyto (in number)	Phyto (in volume)	S-phyto (in number)	S-phyto (in volume)
$R^2$	0.767	0.754	0.739	0.688	0.572	<b>0.865</b>	0.669
(p-value)	( $1.92 \cdot 10^{-6}$ )	( $3.85 \cdot 10^{-6}$ )	( $4.85 \cdot 10^{-6}$ )	( $2.07 \cdot 10^{-5}$ )	( $2.81 \cdot 10^{-4}$ )	( $2.25 \cdot 10^{-8}$ )	( $3.39 \cdot 10^{-5}$ )
Slope	0.796	0.868	0.967	1.201	0.794	<b>1.008</b>	1.091
(p-value)	(0.082)	(0.311)	(0.822)	(0.335)	(0.249)	(0.940)	(0.642)
Intercept	0.035	-0.026	-0.092	-0.261	-0.112	<b>-0.002</b>	-0.193
(p-value)	(0.880)	(0.920)	(0.761)	(0.539)	(0.756)	(0.991)	(0.631)

## 1 **Figures**

2

3 Figure 1: The two different Arrhenius relationships estimated for *Crassostrea gigas* ingestion  
4 rate (grey line) and respiration rate (black line). Arrhenius corrections are given for  
5 temperatures from 3°C to 32 °C. Data from Le Gall and Raillard, 1988; Bougrier et al., 1995;  
6 Ren and Ross, 2000; Mao et al., 2006; and Le Moullac 2008.

7

8 Figure 2: (A) Marennes-Oléron Bay and the location of the experimental study site. (B) The  
9 experimental study site showing the channel system and the oyster ponds.

10

11 Figure 3: The first forcing variable of the model: seawater temperature monitored in the  
12 oyster pond from January 2006 to January 2007, varying from 3°C in January 2006 to 30°C in  
13 July 2006.

14

15 Figure 4: The second forcing variable of the model: food density illustrated through different  
16 food quantifiers monitored in the oyster pond from January 2006 to January 2007: POC (A),  
17 POM (B), chl-a (C) and phytoplankton enumeration (D) expressed in cell number per litre  
18 (black line) and in cumulative cell biovolume ( $\mu\text{m}^3 \text{L}^{-1}$ , grey line). Symbols 1, 2 and 3  
19 indicate common peaks identified in chl-a, POC and POM, whereas symbols from i to viii  
20 indicate peaks which were not identified in all of the food quantifiers.

21

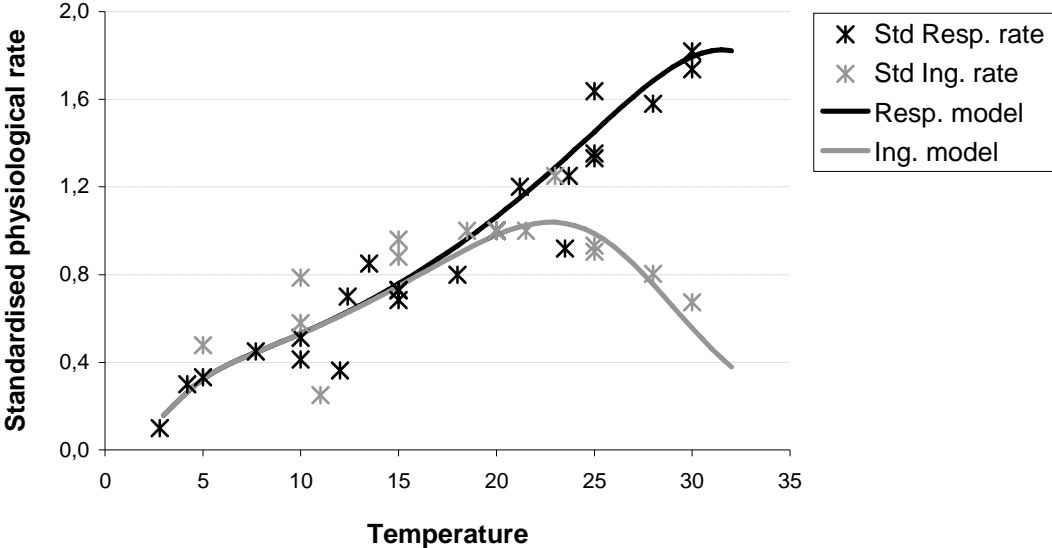
22 Figure 5: Comparisons between observed (symbols, with bars for standard deviation) and  
23 simulated (solid dark line) dry flesh mass, from January 2006 to January 2007, for different  
24 food quantifiers: (A) shows the simulation obtained with POC, (B) with the POM, and (C)  
25 with the chl-a.

26

27 Figure 6: Comparisons between observed (symbols, with bars for standard deviation) and  
28 simulated (solid dark line) dry flesh mass, from January 2006 to January 2007, with  
29 phytoplankton enumeration used as a food quantifier: (A) and (B) show the simulations  
30 obtained using selected phytoplankton composition expressed in number and volume,  
31 respectively, (C) and (D) show the simulations obtained with complete phytoplankton  
32 expressed in number and volume, respectively.

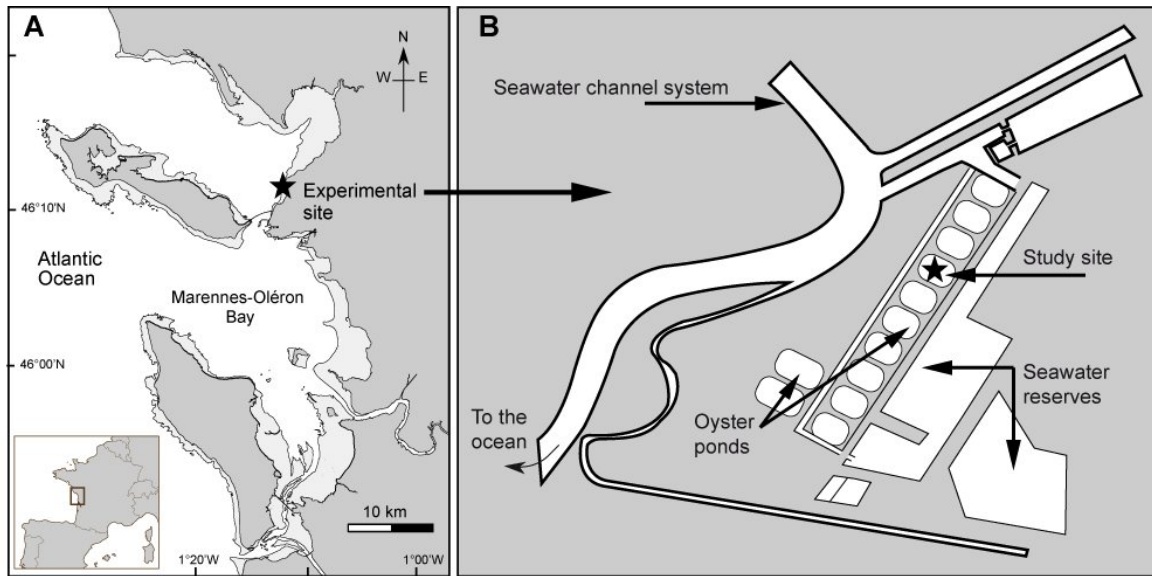
33

1  
2 Figure 1 :



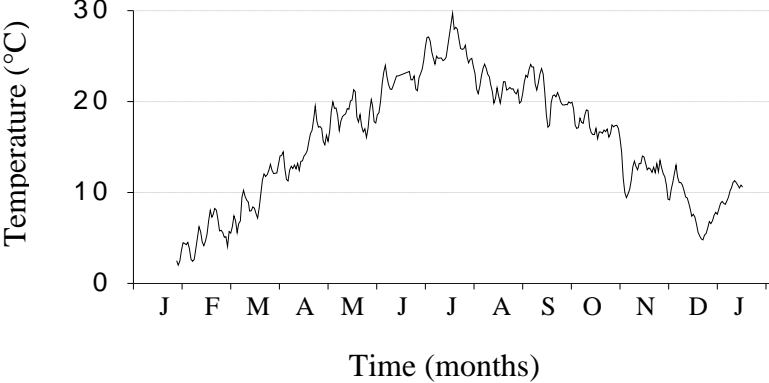
1  
2  
3  
4  
5  
6  
7  
8  
9  
10  
11  
12  
13  
14  
15  
16  
17  
18  
19

Figure 2 :



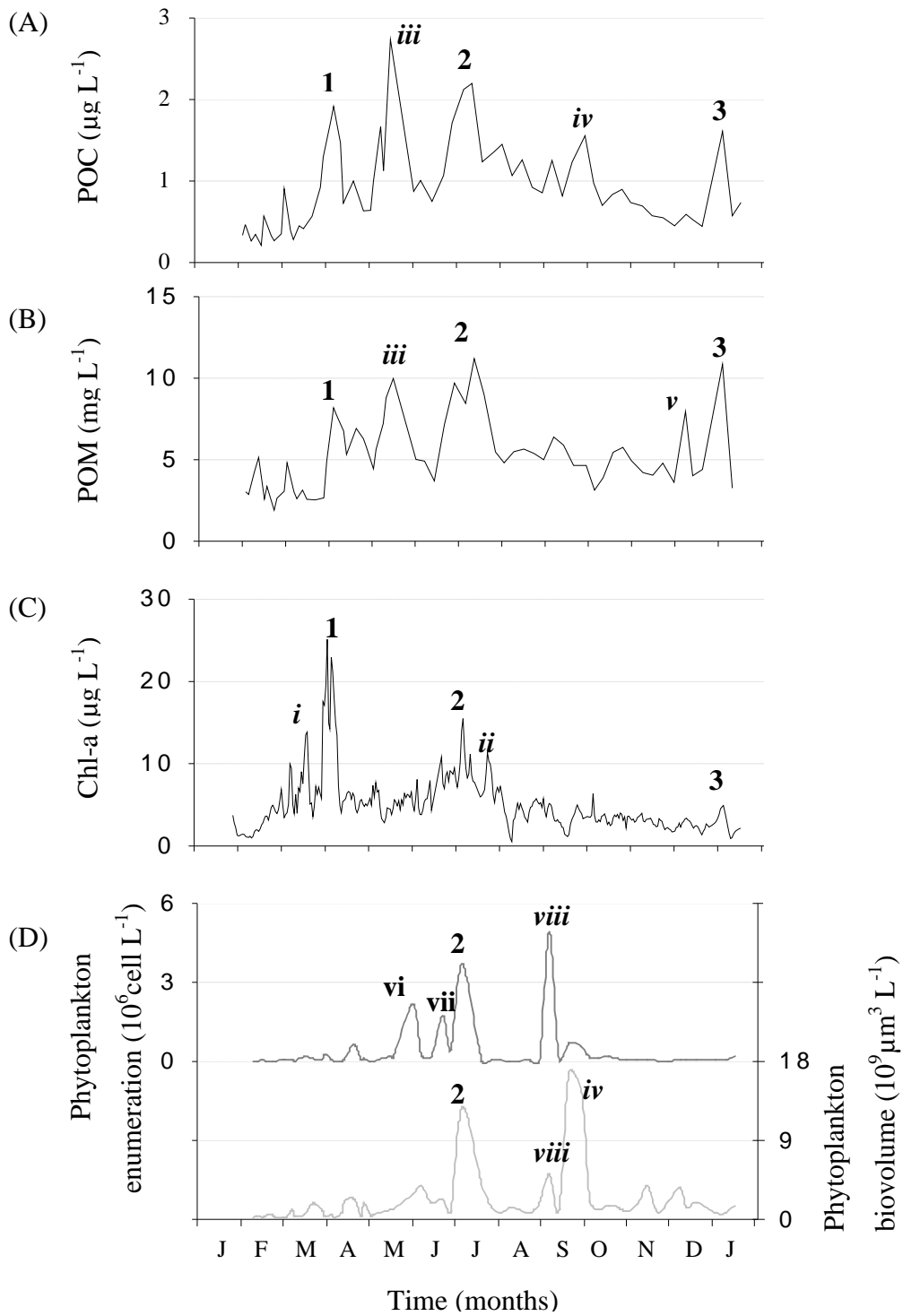
1  
2  
3  
4  
5  
6  
7  
8  
9  
10  
11  
12  
13  
14  
15

Figure 3 :



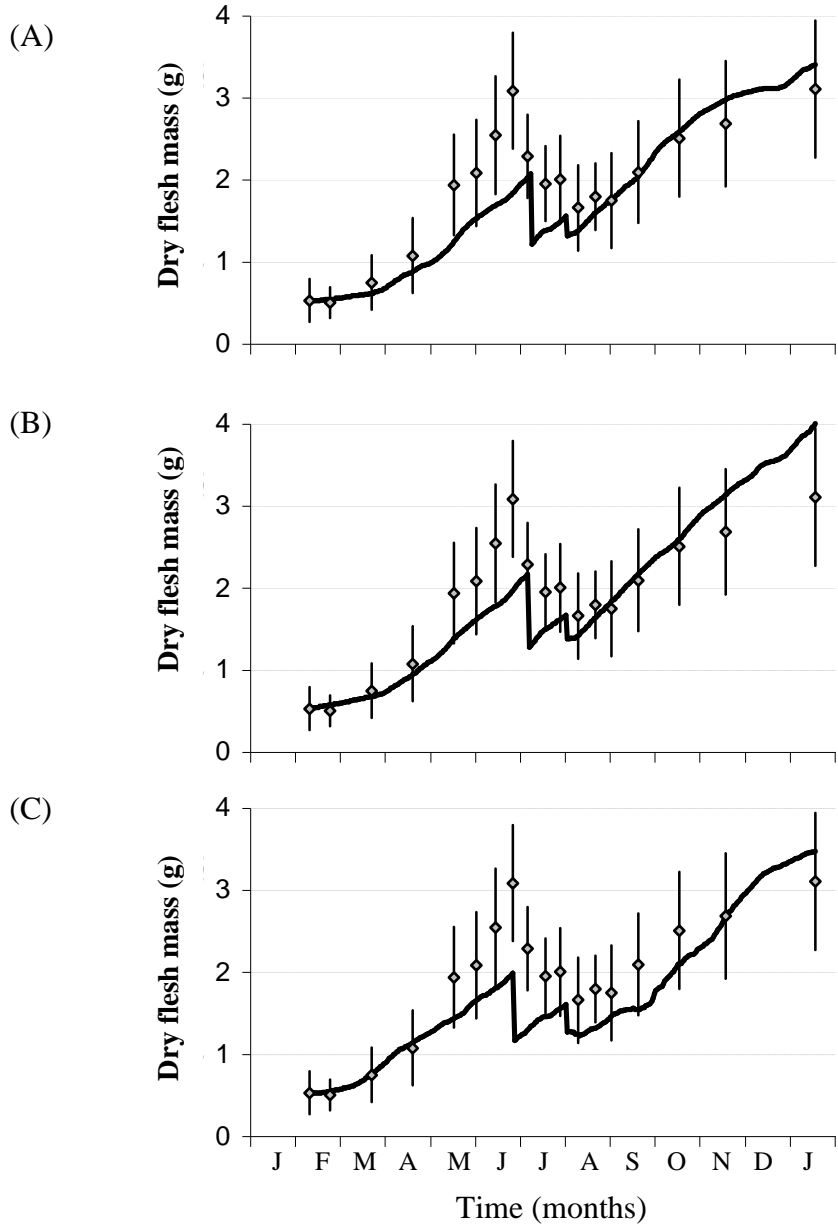
1  
2  
3  
4  
5  
6  
7  
8  
9  
10  
11  
12  
13  
14  
15  
16  
17  
18  
19  
20  
21  
22  
23  
24  
25  
26  
27  
28  
29  
30  
31  
32  
33

Figure 4 :



1  
2  
3  
4  
5  
6  
7  
8  
9  
10  
11  
12  
13  
14  
15  
16  
17  
18  
19  
20  
21  
22  
23  
24  
25  
26  
27  
28  
29  
30

Figure 5 :





1  
2  
3  
4  
5  
6  
7  
8  
9  
10  
11  
12  
13  
14  
15  
16  
17  
18  
19  
20  
21  
22  
23  
24  
25  
26  
27  
28  
29  
30  
31  
32  
33  
34

Figure 6 :

